

Electron density distribution and crystal structure of lithium barium silicate, $\text{Li}_2\text{BaSiO}_4$

Tatsunari Kudo and Yoshinori Hirano

Department of Environmental and Materials Engineering, Nagoya Institute of Technology,
Nagoya 466-8555, Japan

Koichi Momma

Quantum Beam Center, Neutron Scattering Group, National Institute for Materials Science (NIMS),
Ibaraki 305-0044, Japan

Koichiro Fukuda^{a)}

Department of Environmental and Materials Engineering, Nagoya Institute of Technology,
Nagoya 466-8555, Japan

(Received 19 June 2010; accepted 18 July 2010)

Crystal structure of $\text{Li}_2\text{BaSiO}_4$ was reinvestigated by laboratory X-ray powder diffraction. The title compound was hexagonal with space group $P6_3cm$, $Z=6$, unit-cell dimensions $a=0.810\ 408(2)$ nm, $c=1.060\ 829(4)$ nm, and $V=0.603\ 370(3)$ nm³. The initial structural model was successfully derived by the direct methods and further refined by the Rietveld method, with the anisotropic atomic displacement parameters being assigned for all atoms. The reliability indices calculated from the Rietveld refinement were $R_{\text{wp}}=6.72\%$, $S=1.17$, $R_{\text{p}}=5.06\%$, $R_{\text{B}}=1.86\%$, and $R_{\text{F}}=0.98\%$. The maximum-entropy method-based pattern fitting (MPF) method was used to confirm the validity of the structural model, in which conventional structure bias caused by assuming intensity partitioning was minimized. The final reliability indices calculated from MPF were $R_{\text{wp}}=6.74\%$, $S=1.17$, $R_{\text{p}}=5.10\%$, $R_{\text{B}}=1.49\%$, and $R_{\text{F}}=0.69\%$. Atomic arrangements of the final structural model were in excellent agreement with the three-dimensional electron-density distributions determined by MPF. © 2010 International Centre for Diffraction Data.

[DOI: 10.1154/1.3499811]

Key words: lithium barium silicate, X-ray powder diffraction, Rietveld method, maximum-entropy method, electron-density distributions

I. INTRODUCTION

Eu^{2+} -activated $\text{Li}_2(\text{Ca}, \text{Sr}, \text{Ba})\text{SiO}_4$ phosphors are among the most promising silicates for white light-emitting diodes (LEDs) through the integration of blue LED chips because their excitation spectra extend to the longer wavelength region than 460 nm (Saradhi and Varadaraju, 2006; Zhang *et al.*, 2008; He *et al.*, 2008; Kulshreshtha *et al.*, 2009a, 2009b). The crystal structures of the host materials $\text{Li}_2\text{CaSiO}_4$ and $\text{Li}_2\text{SrSiO}_4$ have been well characterized in the literatures (Gard and West, 1973; Hirano *et al.*, 2010). Recently, Kim *et al.* (2009) determined the crystal structure of $\text{Li}_2\text{BaSiO}_4$ [space group $P6_3cm$, $Z=6$, and unit-cell parameters $a=0.810\ 040(1)$ and $c=1.060\ 052(1)$ nm] by synchrotron radiation powder diffraction method for the sample containing impurities. The atomic coordinates of the initial structural model were derived from the direct methods for Ba and Si and the simulated annealing method for O. The positions of Li atoms, which were located near the Ba atoms with the closest distance of 0.327 nm, were determined by the maximum-entropy method (MEM) (Takata *et al.*, 2001). The reliability indices of the refinement were satisfactory. However, the final structural model can still be improved partly

because the interatomic distances do not agree well with those expected from the ionic radii nor bond valence sums. In order to clarify the highly efficient luminescence mechanism and further improve the performance of $\text{Li}_2\text{BaSiO}_4:\text{Eu}^{2+}$ phosphor, a more detailed structural study of the host material will be useful.

A combined use of the Rietveld method (Rietveld, 1967), MEM, and the MEM-based pattern fitting (MPF) method (Izumi *et al.*, 2001) using X-ray powder diffraction (XRPD) data has enabled us to determine three-dimensional (3D) electron-density distributions (EDDs), which efficiently disclose structural details such as precise positions of light atoms near the much heavier ones (Izumi, 2004). The Rietveld method and MEM have a drawback in determining the EDD because the observed structure factors, F_o (Rietveld), are biased toward the structural model assuming intensity partitioning. On the other hand, the MPF method can minimize the structural bias. Thus, the MEM and MPF analyses are alternately repeated (REMEDY cycle) until the reliability indices reach minima. Crystal structures are represented not by structural parameters but by 3D EDD in MPF.

In the present study, we have successfully prepared the powder specimen consisting exclusively of $\text{Li}_2\text{BaSiO}_4$. The coordinates of all atoms, including those of Li, have been readily derived using the direct methods. The validity of the final structural model has been confirmed by the 3D EDD determined by MPF.

^{a)} Author to whom correspondence should be addressed. Electronic mail: fukuda.koichiro@nitech.ac.jp

TABLE I. Crystal data for Li₂BaSiO₄.

Chemical composition	Li ₂ BaSiO ₄
Space group	<i>P</i> 6 ₃ <i>cm</i>
<i>a</i> /nm	0.810 408(2)
<i>c</i> /nm	1.060 829(4)
<i>V</i> /nm ³	0.603 370(3)
<i>Z</i>	6
<i>D_x</i> /Mg m ⁻³	4.02

II. EXPERIMENTAL

A sample of Li₂BaSiO₄ was prepared from stoichiometric amounts of reagent-grade chemicals Li₂CO₃, BaCO₃, and SiO₂. Well-mixed chemicals were pressed into pellets (20 mm diameter and 5 mm thick), heated at 973 K for 3 h, and followed by quenching in air. The procedures of mixing and heating were repeated three times for complete homogenization. The densely sintered pellets were finely ground to obtain a powder specimen.

A diffractometer (X'Pert PRO Alpha-1, PANalytical B.V., Almelo, The Netherlands), equipped with an incident-beam Ge(111) Johansson monochromator to obtain Cu *K*α₁ radiation and a high-speed detector, was used in the Bragg-Brentano geometry. The X-ray generator was operated at 45 kV and 40 mA. A variable divergence slit was used to keep a constant illuminated length of 5 mm on the specimen surface. Other experimental conditions were continuous scan, experimental 2θ range from 10.0114° to 145.3058° (an accuracy of ±0.0001 °2θ), 8097 total data points, and 2.4 h total

experimental time. The structure data were standardized according to rules formulated by Parthé and Gelato (1984) using the computer program STRUCTURE TIDY (Gelato and Parthé, 1987). The crystal-structure models, equidensity iso-surfaces of EDD, and two-dimensional (2D) EDD map were visualized with the computer program VESTA (Momma and Izumi, 2008). Distortion parameters for the coordination polyhedra (Makovicky and Balić-Žunić, 1998) were found using the computer program IVTON (Balić-Žunić and Vickovic, 1996).

III. RESULTS AND DISCUSSION

A. Structure refinement

Peak positions of the experimental diffraction pattern were first determined by finding minima in the second derivatives using the computer program PowderX (Dong, 1999). The 2θ values of 40 observed peak positions were then used as input data to the automatic indexing computer program TREOR90 (Werner *et al.*, 1985). One hexagonal unit cell was found with satisfactory figures of merit: *M*40=217 and *F*40=428 (0.001 673, 56) (de Wolff, 1968; Smith and Snyder, 1979). The derived unit-cell parameters of *a* = 0.810 567(9) and *c* = 1.060 97(2) nm could index all reflections in the observed diffraction pattern.

The observed diffraction peaks were examined to confirm the presence or absence of reflections. Systematic absences *l* ≠ 2*n* for *h* \bar{h} 0*l* reflections were found, suggesting that possible space groups are *P*3*c*1, *P* $\bar{3}$ *c*1, *P*6₃*cm*, *P* $\bar{6}$ *c*2, and *P*6₃/*mcm*. All these space groups were tested and confirmed

TABLE II. Structural parameters and anisotropic atomic displacement parameters (10⁵ × *U*/nm²) for Li₂BaSiO₄.

Site	Wyckoff position	<i>x</i>	<i>y</i>	<i>z</i>	<i>U</i> (eq)	
Li1	6 <i>c</i>	0.2248(31)	0	0.3915(25)	29	
Li2	6 <i>c</i>	0.2730(29)	0	0.0223(24)	24	
Ba	6 <i>c</i>	0.571 50(7)	0	0.2384(7)	19	
Si1	2 <i>a</i>	0	0	0.1540(6)	14	
Si2	4 <i>b</i>	1/3	2/3	0.4838(10)	14	
O1	2 <i>a</i>	0	0	0	9	
O2	4 <i>b</i>	1/3	2/3	0.1366(4)	14	
O3	6 <i>c</i>	0.1900(7)	0	0.2034(8)	21	
O4	12 <i>d</i>	0.2243(6)	0.4477(5)	0.4339(8)	18	
Site	<i>U</i> ₁₁	<i>U</i> ₂₂	<i>U</i> ₃₃	<i>U</i> ₁₂	<i>U</i> ₁₃	<i>U</i> ₂₃
Li1	18(11)	25(14)	45(19)	1/2 <i>U</i> ₂₂	13(11)	0
Li2	29(11)	14(13)	24(16)	1/2 <i>U</i> ₂₂	15(10)	0
Ba	21.7(6)	13.9(6)	19.9(6)	1/2 <i>U</i> ₂₂	-6.0(8)	0
Si1	13.6(22)	<i>U</i> ₁₁	16.0(35)	1/2 <i>U</i> ₁₁	0	0
Si2	10.9(12)	<i>U</i> ₁₁	18.6(23)	1/2 <i>U</i> ₁₁	0	0
O1	9.7(33)	<i>U</i> ₁₁	9.0(72)	1/2 <i>U</i> ₁₁	0	0
O2	11.2(31)	<i>U</i> ₁₁	18.6(54)	1/2 <i>U</i> ₁₁	0	0
O3	22.8(32)	28.5(41)	13.0(71)	1/2 <i>U</i> ₂₂	9.5(29)	0
O4	10.7(35)	21.8(31)	23.8(34)	9.6(27)	9.4(25)	10.4(23)

Note: *U*(eq) is defined as one-third of the trace of the orthogonalized *U*_{*ij*} tensor. The anisotropic displacement factor exponent takes the form $-2\pi^2[h^2a^{*2}U_{11} + k^2b^{*2}U_{22} + l^2c^{*2}U_{33} + 2hka^*b^*U_{12} + 2hla^*c^*U_{13} + 2klb^*c^*U_{23}]$.

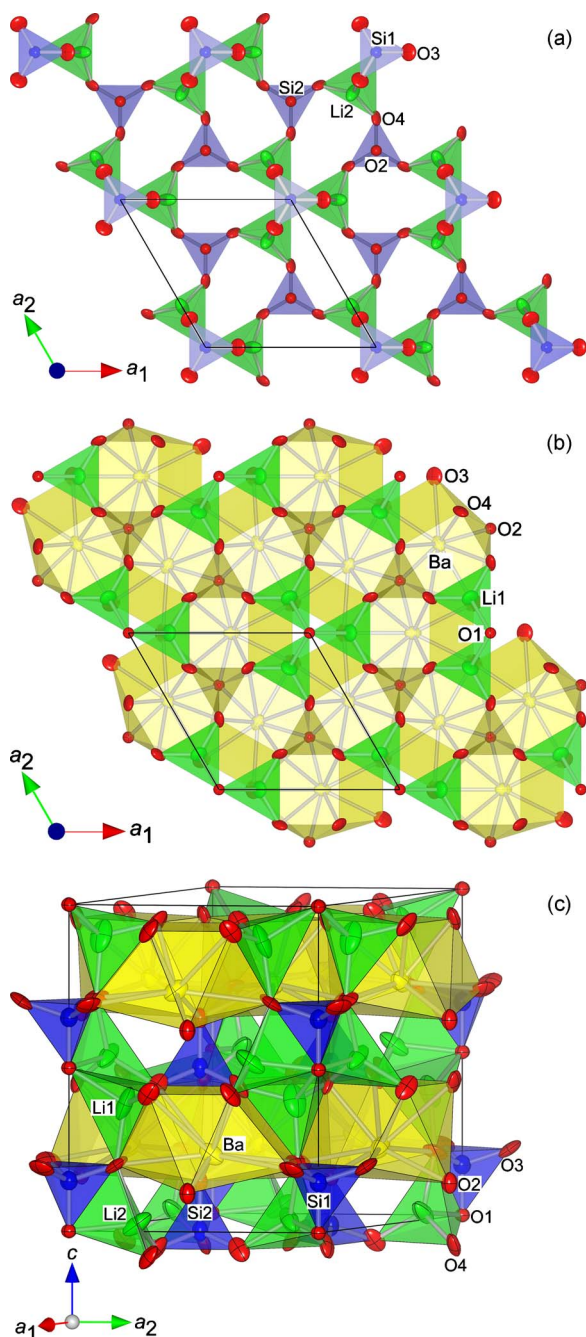


Figure 1. (Color online) Crystal structure of $\text{Li}_2\text{BaSiO}_4$. Two types of basic structural layers (a) $[\text{LiSiO}_4]^{3-}$ and (b) $[\text{LiBaO}_4]^{3-}$ are alternately stacked in the $[001]$ direction to form (c) a three-dimensional structure. Atom numbering corresponds to that given in Table II.

using the EXPO2004 package (Altomare *et al.*, 1999). A unit-cell content with $[12\text{Li } 6\text{Ba } 6\text{Si } 24\text{O}]$ was used as input data for the search of a crystal-structure model. A promising structural model, including two types of coordinates for Li atoms, with the minimum reliability index R_F (Young, 1993) of 7.52% was successfully obtained with the space group $P6_3cm$ in a default run of the program. There were nine independent sites (i.e., two Li sites located at the Wyckoff position $6c$, one Ba site at $6c$, two Si sites at $4b$ and $2a$, and four O sites at $4b$, $6c$, $2a$, and $12d$) in the unit cell. The

derived structural model was isomorphous with that determined by Kim *et al.* (2009).

Structural parameters of all atoms were refined by the Rietveld method using the computer program RIETAN-FP (Izumi and Momma, 2007) with the profile intensity data in the whole 2θ range. A Legendre polynomial with 12 adjustable parameters was fitted to background intensities. The split Pearson VII function (Toraya, 1990) was used to fit the peak profiles. Isotropic atomic displacement parameters (ADPs) were initially assigned to all atoms. The refinement resulted in the reliability (R) indices of $R_{wp}=7.00\%$, $S (=R_{wp}/R_c)=1.22$, $R_p=5.33\%$, $R_B=2.68\%$, and $R_F=1.41\%$ (Young, 1993). We subsequently assigned anisotropic ADPs to obtain the lower R indices of $R_{wp}=6.72\%$, $S=1.17$, $R_p=5.06\%$, $R_B=1.86\%$, and $R_F=0.98\%$. Crystal data are given in Table I, and the final atomic positional parameters and anisotropic ADPs are given in Table II. The ratio of the largest/smallest principal ADP components of all atoms were necessarily less than 2.44, indicating that the refinement was entirely successful to obtain the reasonable structural model (Figure 1). The two types of Li sites have been found to be located close to the Ba site: the interatomic distance of Li1-Ba was 0.325(1) nm and that of Li2-Ba was 0.333(2) nm.

The EDDs with $162 \times 162 \times 212$ pixels in the unit cell, the spatial resolution of which is approximately 0.005 nm, were obtained from the MPF method using the computer programs RIETAN-FP and PRIMA (Izumi and Dilanian, 2002). After one REMEDY cycle, R_B and R_F further decreased to 1.49% and 0.69%, respectively ($R_{wp}=6.74\%$, $S=1.17$, and $R_p=5.10\%$). Subtle EDD changes as revealed by MPF significantly improve the R_B and R_F indices. The decreases in R indices demonstrate that the crystal structure can be seen more clearly from EDD instead of from the conventional structural parameters reported in Table II. Observed, calculated, and difference XRPD patterns for the final MPF are plotted in Figure 2.

The individual equidensity isosurfaces of 3D EDD in Figure 3 are in reasonably good agreement with the corresponding atom arrangements in Figure 1(c). Bonding electrons for highly covalent bonds (Si-O) are clearly visualized; the representation of these bonds by 3D EDD must contribute to the decrease in R_B . The 2D EDD map at the height of Li1, Li2, Ba, Si1, O1, and O3 sites shows that the positions of Li atoms are successfully disclosed by the EDD (Figure 4). We found the peak positions of EDD from the 3D pixel data and compared them with the coordinates of all atoms that were determined by the Rietveld method. The positional deviations of all atoms in the unit cell were found to be necessarily less than 0.003 nm, which is within the resolution limit of the 3D EDD. We therefore concluded that the present structural model would reasonably and satisfactorily represent the crystal structure of $\text{Li}_2\text{BaSiO}_4$.

B. Structure description

Selected interatomic distances and bond angles, together with their standard deviations, are listed in Table III. The average Li-O bond lengths are 0.198 nm for Li_1O_4 and 0.201 nm for Li_2O_4 , which are comparable to those of the LiO_4 tetrahedra in $\text{La}_2\text{SrSiO}_4$ (0.198 nm), $\text{Li}_2\text{EuSiO}_4$ (0.198 nm),

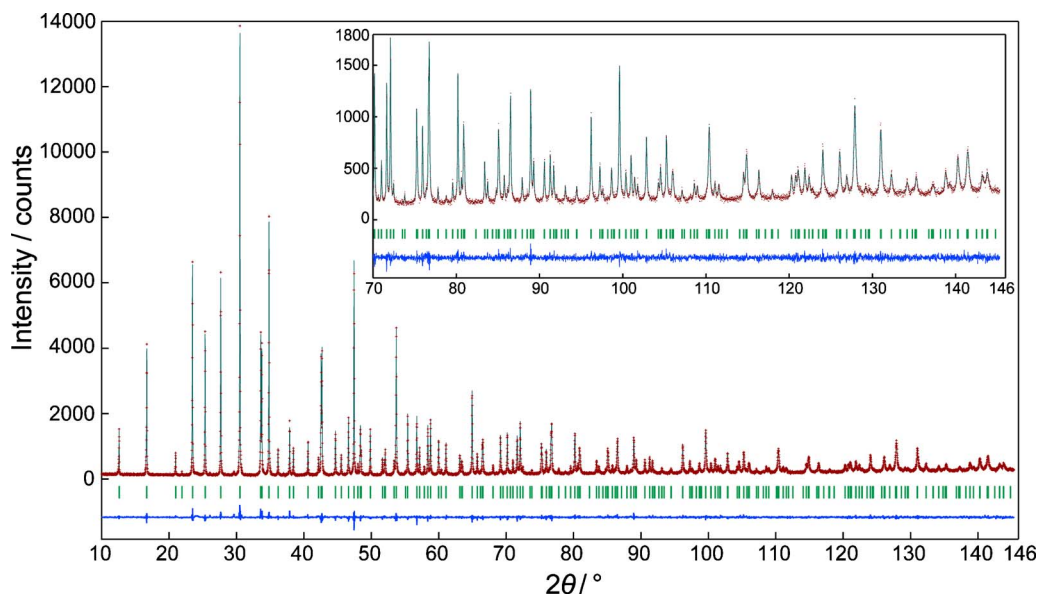


Figure 2. (Color online) Comparison of the observed diffraction pattern of $\text{Li}_2\text{BaSiO}_4$ (symbol: +) with the corresponding calculated pattern (upper solid line). The difference curve is shown in the lower part of the diagram. Vertical bars indicate the positions of possible Bragg reflections.

and $\text{Li}_2\text{CaSiO}_4$ (0.197 nm) (Hirano *et al.*, 2010; Haferkorn and Meyer, 1998; Gard and West, 1973). When the volume distortion parameters v are compared between the two types of tetrahedra Li1O_4 and Li2O_4 , the extent of distortion (v value) is smaller for the former than for the latter (Table IV). The average Si-O bond lengths of 0.163 nm for Si1O_4 and 0.162 nm for Si2O_4 agree well with the interatomic distance of 0.164 nm calculated from the ionic radii of Si^{4+} and O^{2-} in the fourfold coordination [$r(\text{Si}^{4+}(4))=0.026$ nm and $r(\text{O}^{2-}(4))=0.138$ nm] (Shannon, 1976). The average values of the O-Si-O angles are 109.5° . These interatomic distance and bond angle are in good agreement with those found in

other silicates (Baur, 1971). The BaO_9 polyhedron showed the bond lengths ranging from 0.264 to 0.323 nm. Ionic radii of Ba^{2+} in the ninefold coordination [$r(\text{Ba}^{2+}(9))=0.147$ nm and $r(\text{O}^{2-}(8))=0.142$ nm] predict the interatomic distance of 0.289 nm for Ba-O. This predicted value is in good agreement with the corresponding average interatomic distance of 0.293 nm. Valence bond sums calculated on the basis of bond-strength analysis (Li1: 1.06, Li2: 0.97, Ba: 1.96, Si1: 3.95, and Si2: 3.98) are in good agreement with the expected

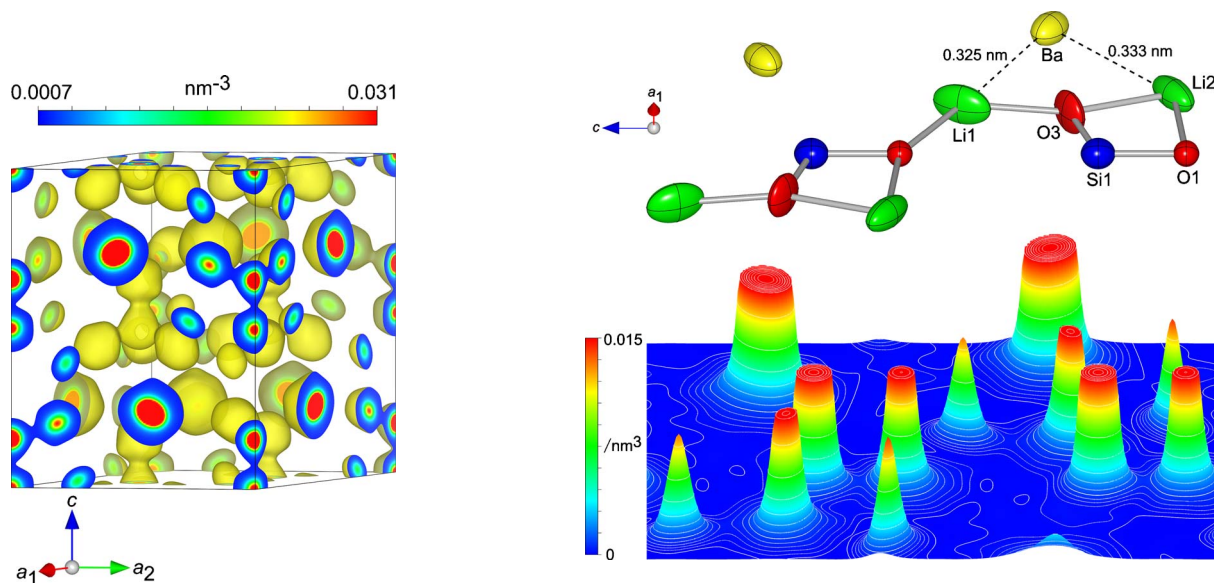


Figure 3. (Color online) Three-dimensional electron-density distributions determined by MPF. Isosurfaces expressed in smooth shading style for an equidensity level of 0.0007 nm^{-3} .

Figure 4. (Color online) A bird's eye view of electron densities up to 3.0% of the maximum (0.512 nm^{-3}) on the (100) plane (lower part) with the corresponding atomic arrangements (upper part). Atom numbering corresponds to that given in Table II.

TABLE III. Selected bond lengths (nm) and angles (deg) in $\text{Li}_2\text{BaSiO}_4$.

Li1-O4	0.1867(14) × 2
Li1-O3	0.2015(27)
Li1-O1	0.2155(23)
⟨Li1-O⟩	0.198
O1-Li1-O3	114.2(13)
O1-Li1-O4	106.1(8) × 2
O3-Li1-O4	107.8(8) × 2
O4-Li1-O4	114.9(14)
⟨O-Li1-O⟩	109.4
Li2-O4	0.1898(12) × 2
Li2-O3	0.2036(22)
Li2-O1	0.2225(25)
⟨Li2-O⟩	0.201
O1-Li2-O3	76.8(7)
O1-Li2-O4	102.4(10) × 2
O3-Li2-O4	123.8(6) × 2
O4-Li2-O4	111.5(10)
⟨O-Li2-O⟩	106.8
Si1-O1	0.1633(6)
Si1-O3	0.1627(6) × 3
⟨Si1-O⟩	0.163
O1-Si1-O3	108.8(3) × 3
O3-Si1-O3	110.1(3) × 3
⟨O-Si1-O⟩	109.5
Si2-O2	0.1620(7)
Si2-O4	0.1625(3) × 3
⟨Si2-O⟩	0.162
O2-Si2-O4	109.0(3) × 3
O4-Si2-O4	109.9(3) × 3
⟨O-Si2-O⟩	109.5
Ba-O2	0.2641(2) × 2
Ba-O3	0.3037(1) × 2
Ba-O3	0.3114(6)
Ba-O4	0.2706(4) × 2
Ba-O4	0.3230(5) × 2
⟨Ba-O⟩	0.293

formal oxidation states of Li^+ , Ba^{2+} , and Si^{4+} ions (Brown and Altermatt, 1985; Brese and O’Keeffe, 1991). The average bond lengths of Li-O, Si-O, and Ba-O are in agreement with those expected from the bond valence sums (Li-O: 0.1979 nm, Si-O: 0.1624 nm, and Ba-O: 0.2847 nm).

The crystal structure of lithium barium silicate consists of the five types of polyhedra, LiIO_4 , Li_2O_4 , SiIO_4 , Si_2O_4 ,

and BaO_9 . Three Li_2O_4 tetrahedra and one SiIO_4 tetrahedron are connected via O1-O3 edges to form a $[\text{Li}_3\text{SiO}_{10}]^{13-}$ unit. Individual units are further linked through Si_2O_4 tetrahedra to form a basic structural layer $[\text{LiSiO}_4]^{3-}$ parallel to (001) [Figure 1(a)]. The BaO_9 polyhedra mutually share faces O2-O3-O4 to form a two-dimensional sheet with the composition $[\text{Ba}_3\text{O}_{11}]^{16-}$. Three LiIO_4 tetrahedra are linked via O1 vertexes to form a $[\text{Li}_3\text{O}_{10}]^{17-}$ unit. The $[\text{Li}_3\text{O}_{10}]^{17-}$ units and $[\text{Ba}_3\text{O}_{11}]^{16-}$ sheet are joined by sharing faces O3-O4-O4 to build up the other basic layer $[\text{LiBaO}_4]^{5-}$ parallel to (001) [Figure 1(b)]. These two types of basic layers are alternately stacked in the [001] direction with two layers each per unit cell to form a three-dimensional structure [Figure 1(c)].

We compared the present structural model with that determined by Kim *et al.* (2009) to find that the unit-cell dimensions as well as the coordinates of relatively heavy atoms such as Ba, Si, and O were almost comparable between the two structures. For example, the distances from O1 atoms, which are located at the origin of the coordinate axes, to Ba atoms were 0.4296(4) nm for the former structural model and 0.4346(14) nm for the latter, with the deviation being less than 1.3%. On the other hand, the coordinates of Li atoms were quite different; the Li1-O1 and Li2-O1 distances determined in the present study (Table III) were longer than those of the previous study by 12.6% and 9.1%, respectively.

IV. CONCLUSION

We successfully refined the crystal structure of lithium barium silicate $\text{Li}_2\text{BaSiO}_4$, having a hexagonal unit cell with space group $P6_3cm$. The basic structural layers of the crystal structure were $[\text{LiSiO}_4]^{3-}$ and $[\text{LiBaO}_4]^{5-}$, comprising five types of polyhedra, LiIO_4 , Li_2O_4 , SiIO_4 , Si_2O_4 , and BaO_9 . These two types of basic layers were alternately stacked in the [001] direction with two layers each per unit cell to form a three-dimensional structure. The validity of this structural model was confirmed by the EDD determined by MPF. The 2D EDD map at the height of Li sites showed that the positions of Li atoms were successfully disclosed by the EDD.

TABLE IV. Polyhedral distortion parameters.

Polyhedron	Distortion parameters					
	Δ/nm	r_s/nm	V_s/nm^3	σ	V_p/nm^3	v
LiIO_4	0.109	0.198	0.0327	1	0.0039	0.020
Li_2O_4	0.127	0.198	0.0323	1	0.0036	0.081
SiIO_4	0.003	0.163	0.0181	1	0.0022	0.000
Si_2O_4	0.002	0.162	0.0179	1	0.0022	0.000
BaO_9	0.052	0.291	0.1027	0.919	0.0409	0.184

Note: Δ =eccentricity; r_s =radius of sphere fitted to ligands; V_s =sphere volume; σ =sphericity; V_p =volume of coordination polyhedron; v =volume distortion; and σ for coordination number four is 1 by definition.

- Altomare, A., Burla, M. C., Camalli, M., Carrozzini, B., Cascarano, G. L., Giacovazzo, C., Guagliardi, A., Moliterni, A. G. G., Polidori, G., and Rizzi, R. (1999). "EXPO: A program for full powder pattern decomposition and crystal structure solution," *J. Appl. Crystallogr.* **32**, 339–340.
- Balić-Žunić, T. and Vickovic, I. (1996). "IVTON—Program for the calculation of geometrical aspects of crystal structures and some crystal chemical applications," *J. Appl. Crystallogr.* **29**, 305–306.
- Baur, W. H. (1971). "Prediction of bond length variations in silicon-oxygen bonds," *Am. Mineral.* **56**, 1573–1599.
- Brese, N. E. and O'Keeffe, M. (1991). "Bond-valence parameters for solids," *Acta Crystallogr., Sect. B: Struct. Sci.* **47**, 192–197.
- Brown, I. D. and Altermatt, D. (1985). "Bond-valence parameters obtained from a systematic analysis of the inorganic crystal structure database," *Acta Crystallogr., Sect. B: Struct. Sci.* **41**, 244–247.
- de Wolff, P. M. (1968). "A simplified criterion for the reliability of a powder pattern indexing," *J. Appl. Crystallogr.* **1**, 108–113.
- Dong, C. (1999). "POWDERX: Windows-95-based program for powder x-ray diffraction data processing," *J. Appl. Crystallogr.* **32**, 838.
- Gard, J. A. and West, A. R. (1973). "Preparation and crystal structure of $\text{Li}_2\text{CaSiO}_4$ and isostructural $\text{Li}_2\text{CaGeO}_4$," *J. Solid State Chem.* **7**, 422–427.
- Gelato, L. M. and Parthé, E. (1987). "STRUCTURE TIDY—A computer program to standardize crystal structure data," *J. Appl. Crystallogr.* **20**, 139–143.
- Haferkorn, B. and Meyer, G. (1998). " $\text{Li}_2\text{EuSiO}_4$, an europium(II) lithosilicate. $\text{Eu}[(\text{Li}_2\text{Si})\text{O}_4]$," *Z. Anorg. Allg. Chem.* **624**, 1079–1081.
- He, H., Fu, R., Wang, H., Song, X., Pan, Z., Zhao, X., Zhang, X., and Cao, Y. (2008). " $\text{Li}_2\text{SrSiO}_4:\text{Eu}^{2+}$ phosphor prepared by the Pechini method and its application in white light emitting diode," *J. Mater. Res.* **23**, 3288–3294.
- Hirano, Y., Iwata, T., Momma, K., and Fukuda, K. (2010). "Electron density distribution and crystal structure of lithium strontium silicate, $\text{Li}_2\text{SrSiO}_4$," *Powder Diffr.* **25**, 4–8.
- Izumi, F. (2004). "Beyond the ability of Rietveld analysis: MEM-based pattern fitting," *Solid State Ionics* **172**, 1–6.
- Izumi, F. and Dilanian, R. A. (2002). *Recent research developments in physics* (Transworld Research Network—Trivandrum, Trivandrum, India), Vol. 3, Pt. II, pp. 699–726.
- Izumi, F., Kumazawa, S., Ikeda, T., Hu, W.-Z., Yamamoto, A., and Oikawa, K. (2001). "MEM-based structure-refinement system REMEDY and its applications," *Mater. Sci. Forum* **378–381**, 59–64.
- Izumi, F. and Momma, K. (2007). "Three-dimensional visualization in powder diffraction," *Solid State Phenom.* **130**, 15–20.
- Kim, J., Ahn, D., Kulshreshtha, C., Sohn, K.-S., and Shin, N. (2009). "Lithium barium silicate, $\text{Li}_2\text{BaSiO}_4$, from synchrotron powder data," *Acta Crystallogr., Sect. C: Cryst. Struct. Commun.* **65**, i14–i16.
- Kulshreshtha, C., Sharma, A. K., and Sohn, K.-S. (2009a). "Effect of local structures on the luminescence of $\text{Li}_2(\text{Sr}, \text{Ca}, \text{Ba})\text{SiO}_4:\text{Eu}^{2+}$," *J. Electrochem. Soc.* **156**, J52–J56.
- Kulshreshtha, C., Shin, N., and Sohn, K.-S. (2009b). "Decay behavior of $\text{Li}_2(\text{Sr}, \text{Ba}, \text{Ca})\text{SiO}_4:\text{Eu}^{2+}$ phosphors," *Electrochem. Solid-State Lett.* **12**, J55–J57.
- Makovicky, E. and Balić-Žunić, T. (1998). "New measure of distortion for coordination polyhedra," *Acta Crystallogr., Sect. B: Struct. Sci.* **54**, 766–773.
- Momma, K. and Izumi, F. (2008). "VESTA: A three-dimensional visualization system for electronic and structural analysis," *J. Appl. Crystallogr.* **41**, 653–658.
- Parthé, E. and Gelato, L. M. (1984). "The standardization of inorganic crystal-structure data," *Acta Crystallogr., Sect. A: Found. Crystallogr.* **40**, 169–183.
- Rietveld, H. M. (1967). "Line profiles of neutron powder-diffraction peaks for structure refinement," *Acta Crystallogr.* **22**, 151–152.
- Saradhi, M. P. and Varadaraju, U. V. (2006). "Photoluminescence studies on Eu^{2+} -activated $\text{Li}_2\text{SrSiO}_4$ —A potential orange-yellow phosphor for solid-state lighting," *Chem. Mater.* **18**, 5267–5272.
- Shannon, R. D. (1976). "Revised effective ionic radii and systematic studies of interatomic distances in halides and chalcogenides," *Acta Crystallogr., Sect. A: Cryst. Phys., Diffr., Theor. Gen. Crystallogr.* **32**, 751–767.
- Smith, G. S. and Snyder, R. L. (1979). " F_N : A criterion for rating powder diffraction patterns and evaluating the reliability of powder-pattern indexing," *J. Appl. Crystallogr.* **12**, 60–65.
- Takata, M., Nishibori, E., and Sakata, M. (2001). "Charge density studies utilizing powder diffraction and MEM. Exploring of high T_c superconductors, C60 superconductors and manganites," *Z. Kristallogr.* **216**, 71–86.
- Toraya, H. (1990). "Array-type universal profile function for powder pattern fitting," *J. Appl. Crystallogr.* **23**, 485–491.
- Werner, P. E., Eriksson, L., and Westdahl, M. (1985). "TREOR, a semi-exhaustive trial-and-error powder indexing program for all symmetries," *J. Appl. Crystallogr.* **18**, 367–370.
- Young, R. A. (1993). *The Rietveld Method*, edited by R. A. Young (Oxford University Press, Oxford, U.K.), pp. 1–38.
- Zhang, X., He, H., Li, Z., Yu, T., and Zou, Z. (2008). "Photoluminescence studies on Eu^{2+} and Ce^{3+} -doped $\text{Li}_2\text{SrSiO}_4$," *J. Lumin.* **128**, 1876–1879.